Journal Pre-proof

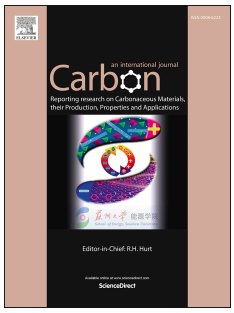

The voltage-dependent manipulation of few-layer graphene with a scanning tunneling microscopy tip

Mona M. Alyobi, Chris J. Barnett, Cyrill B. Muratov, Vitaly Moroz, Richard J. Cobley

PII: S0008-6223(20)30294-3

DOI: https://doi.org/10.1016/j.carbon.2020.03.046

Reference: CARBON 15185

To appear in: *Carbon*

Received Date: 4 February 2020

Revised Date: 13 March 2020

Accepted Date: 23 March 2020

Please cite this article as: M.M. Alyobi, C.J. Barnett, C.B. Muratov, V. Moroz, R.J. Cobley, The voltage-dependent manipulation of few-layer graphene with a scanning tunneling microscopy tip, *Carbon* (2020), doi: https://doi.org/10.1016/j.carbon.2020.03.046.

This is a PDF file of an article that has undergone enhancements after acceptance, such as the addition of a cover page and metadata, and formatting for readability, but it is not yet the definitive version of record. This version will undergo additional copyediting, typesetting and review before it is published in its final form, but we are providing this version to give early visibility of the article. Please note that, during the production process, errors may be discovered which could affect the content, and all legal disclaimers that apply to the journal pertain.

© 2020 Published by Elsevier Ltd.

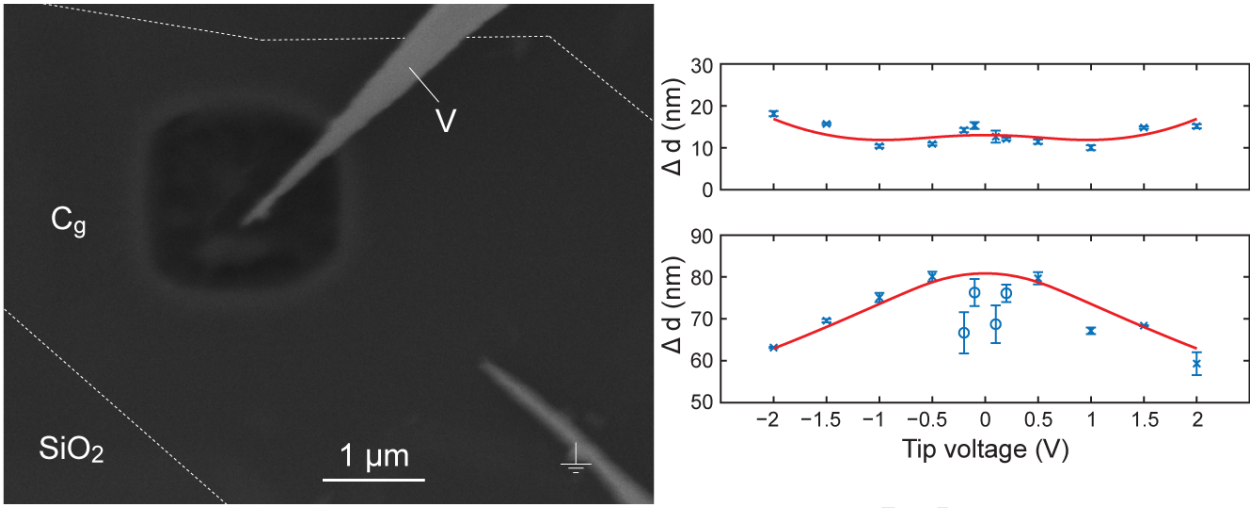

Journal Pre-proof

The voltage-dependent manipulation of few-layer graphene with a scanning tunneling microscopy tip

Journal Pre-proof

Mona M. Alyobi[1], Chris J. Barnett[1], Cyrill B. Muratov[2], Vitaly Moroz[3], Richard J. Cobley[1*].

[1] College of Engineering, Swansea University, Bay Campus, Fabian Way, Swansea, SA1 8EN, UK.

[2] Department of Mathematical Sciences, New Jersey Institute of Technology, University Heights, Newark, NJ 07102, US.

[3] Department of Mathematics, Swansea University, Bay Campus, Fabian Way, Swansea, SA1 8EN, UK.

Abstract

Strain and deformation alter the electronic properties of graphene, offering the possibility to control its transport behavior. The tip of a scanning tunneling microscope is an ideal tool to mechanically perturb the system locally while simultaneously measuring the electronic response. Here we stretch few- and multi-layer graphene membranes supported on SiO_2 substrates and suspended over voids. An automated approach-retraction method stably traces the graphene deflection hysteresis curve hundreds of times across four samples, measuring the voltage-dependent stretching, from which we extract the hysteresis width. Using a force-balance model, we are able to reproduce the voltage-dependent hysteretic graphene extension behavior. We directly observe a voltage-dependent interplay where electrostatic forces dominate at high voltage and van der Waals forces at low voltage. The relative contribution of each force is dependent on the graphene and tunneling resistance, giving rise to different observed voltage-dependent behavior between samples. Understanding the voltage dependence of these forces impacts scanning probe measurement of 2D materials and informs oscillating graphene device design where similar forces act from the side walls of cavities, leading towards strain engineering of layered 2D systems.

Journal Pre-proof

1. Introduction

Journal Pre-proof

Controlling the strain in graphene offers a way to tailor its electronic properties, with repeated manipulation expected to lead to 2D van der Waals heterostructures [1-4]. Scanning tunneling microscopy (STM) is an ideal tool to both measure and manipulate graphene and other 2D materials by using the interaction of the probe to pull and push the graphene layers, simultaneously loading and measuring the electronic response [5-7]. As well as inducing and stretching ripples normal to the graphene plane, STM can also be used to perform stress-strain measurements on graphene, offering greater insights into its behavior when used in flexible electronics [8, 9].

When a probe is moved towards suspended or supported graphene, attractive forces cause the graphene membrane to deflect or 'snap' discontinuously up to the tip [2, 6, 7, 10]. For single layer graphene this forms a nanoscale bi-stable electromechanical system where the STM probe can be used to perturb the system between the in-contact deflected, and out-of-contact relaxed states. For few-layer graphene, the tip approach exhibits similar behavior but in retraction the layers may detach one at a time [6], as competing forces cause the graphene to 'snap' discontinuously back to the substrate [9]. Although atomic force microscopy (AFM) can be used to perform indentation measurements on graphene, it may not be suited to retraction stretching of graphene, because the graphene-tip forces deflect an AFM cantilever down to the graphene instead of deflecting the graphene up to the probe [11].

Understanding how strain and deformation in 2D materials alters the electronic transport is critical to integrating them into devices [12, 13]. Graphene can form resonators for ultra-sensitive detection, but short-range and electrostatic forces alter the static deflection, substrate bonding, side wall interaction and other vibration properties [14-16]. Few-layer graphene is less affected by substrate and impurity effects and can reduce some of these detrimental strain effects [17, 18].

When studying the electronic properties, the lithographic formation of contacts can contaminate the sample, particularly any residual resist [19-21]. Direct probe contact to nano-materials instead provides a local, non-destructive and comparably fast technique for electronic transport measurements [22-24].

In STM the tip exerts both short-range van der Waals and long-range electrostatic forces to manipulate the graphene hysteretically between the two stable states [7]. The electrostatic component of the force is voltage-dependent, while van der Waals is not, yet there has been little experimental work investigating the voltage dependence of this combined effect, nor modelling how voltage affects the interplay of the two forces and the effect on how far graphene can be stretched. We use here an automated method to repeatedly perturb the graphene hysteretically hundreds of times and extract the hysteresis width. By varying the voltage between each measurement we are able to extract the graphene extension as a function of voltage.

2. Methods

2.1 Experimental

Journal Pre-proof

Highly-oriented pyrolytic graphite was mechanically exfoliated on to a 90 nm layer of SiO_2 on Si grown by thermal oxidation and calibrated by ellipsometry. Holes in the silicon substrate were patterned by electron beam lithography and plasma etched prior to oxidation and graphene deposition [25]. Flakes were identified using scanning electron microscopy, then thickness and quality was confirmed by Raman microscopy and AFM [6]. Samples were annealed at 200 °C for an hour in situ in an Omicron multi-probe ultra high vacuum system, then contacted and measured as described in the text using electrochemically etched tungsten tips which were annealed in vacuum to remove surface oxide [26]. More information is available in the Supplementary Data File (see Appendix A). Each force-release measurement was repeated using an automatic script to maintain the same approach and retraction speed. This was repeated for all voltages shown at the same point on the same sample, and then the whole process repeated again on each of the four samples.

2.2 Theoretical

The elastic force $F_{Elastic}$ is modeled as an effective Hookean spring with displacement d_1 and spring constant k. The van der Waals force F_{vdW} is modeled by a formula for the interaction of a sphere of radius a with a plane separated from the sphere by distance $d_0 \lesssim a$, with Hamaker constant A and an effective offset d_{vdW} introduced to account for the surface roughness of the probe surface. The electrostatic force $F_{Elec.}$ is modelled as the force between a sphere of radius a held at potential V_0 at distance $d_0 \lesssim a$ relative to a grounded plane, with an effective offset $d_{Elec.}$ to similarly account for surface roughness. The electrostatic force $F_{Elec.}$ depends on the potential difference V_0 between the probe and the graphene sheet, which is found by considering an equivalent electric circuit for the assembly where the graphene resistance R_G is in series with the combined tip and tunneling resistance R_T. The tunnel resistance is assumed to depend exponentially on the distance between the probe and graphene sheet. The three forces are then balanced for $F_{Elast} = F_{vdW} + F_{Elec.}$ where the non-linear feedback produces hysteretic responses. More information is given in the Supplementary Data File (see Appendix A).

3. Results

3.1 Manipulating graphene with STM

We use a dual tip method where mechanically exfoliated pristine graphene is contacted directly with one STM tip to provide ground, using the second STM tip in tunneling contact to manipulate and characterize the sample. Suspended and supported few-layer (n=6) and multi-layer (n~8) graphene on 90 nm SiO_2 on Si are contacted by tips guided by scanning electron microscopy (SEM), all within ultra high vacuum (see Supplementary Data File, Appendix A). By repeatedly measuring the hysteretic behavior at different voltages, we observe a complex non-linear voltage dependence.

Journal Pre-proof

Fig. 1a shows two STM probes positioned on a flake of few-layer (n=6) graphene. The bottom right probe is in direct mechanical contact with the graphene and held at ground to provide an electrical path for the graphene which would otherwise be electrically floating on the insulating substrate [27]. To aid the eye, dashed white lines show the edge of the flake. The top probe is just out of tunneling contact from the portion of graphene suspended over a ~1 μm ×1 μm hole in the SiO_2 layer and moves toward and away from the graphene in the normal z-direction. A schematic of the hysteretic tip interaction with the graphene during approach and retraction is shown in Fig. 1b with labels matching an example tunneling current measurement in Fig. 1c.

For all measurements the probe starts out of contact then moves at a constant speed towards the graphene in region A (z becoming negative) with the measured tunneling current remaining negligible. At point B all six layers of the graphene discontinuously deflects upwards to meet the approaching probe. The probe can continue to approach with increasing current (shown in gray), before retracting in region C where six discontinuous current drops are observed. When repeated, these discontinuities occur at the same current and z height and the number matches the number of graphene sheets measured with AFM and Raman. Further, the resistance of each layer detaching from the probe corresponds to a sequential 1/R parallel resistance reduction. In previous work we have modelled these current drops and shown they correspond to the detachment of graphene from the tip, layer by layer [6]. At point D the last graphene layer detaches from the probe and the current returns to zero, with the probe continuing to retract into region E.

Although the graphene initially attaches to the probe at point B, during retraction it is deflected or stretched upwards beyond this point, before restoring mechanical forces cause it to detach from the probe at point D. This hysteresis is common in similar STM graphene manipulation studies [7]. We define the stretch of the graphene being between the point at which the graphene initially contacts the probe and the point at which the graphene fully detaches from the probe, indicated in Fig. 1c, as Δd. Our method is classified as feedback-off I(z) measurements with a fixed voltage V, where I is the tunneling current and z the out-of-plane displacement of the probe. This creates point ripples – radially symmetric upward displacement of the graphene – sometimes termed "local centrosymmetric bubbles" [3], instead of extending lateral folds or wrinkles. By scripting the approach and retraction measurements within the STM control system we are able to repeatedly measure these hysteresis curves and investigate the voltage dependence of the hysteresis width across four different samples.

Journal Pre-proof

Journal Pre-proof

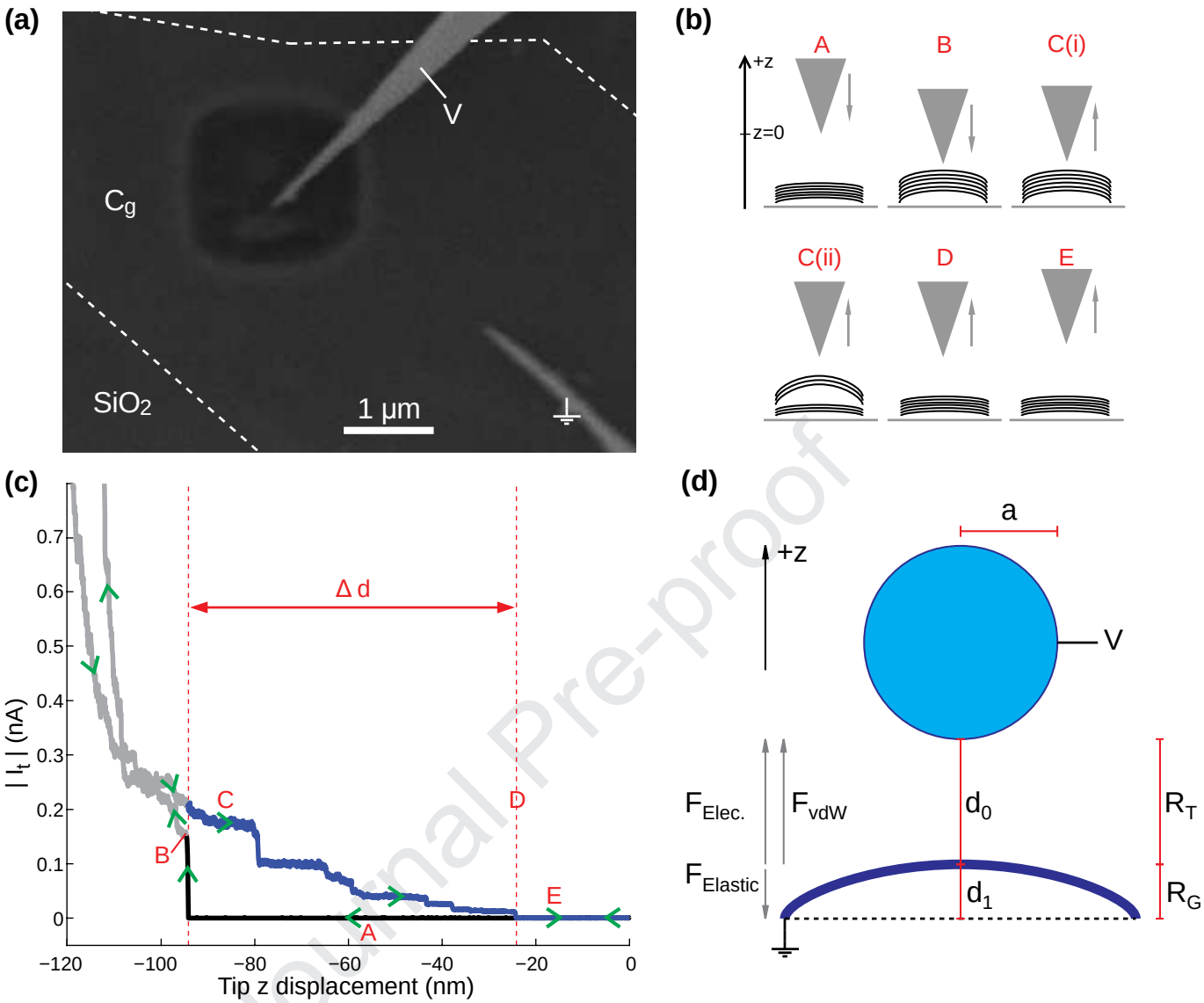

Fig. 1. *(a) SEM image of two tips positioned over few-layer (n=6) graphene on SiO_2. Bottom right tip at ground and in contact with the graphene, upper tip just out of tunneling contact with the portion of the graphene suspended over a hole in the substrate. Dashed lines mark the boundary of the graphene flake on the SiO_2 substrate. (b) Schematic diagram of the approach and retraction phases with matching labels. (c) example approach-retraction STM measurement truncated at 0.8 nA for V_{tip} = +0.01 V. (d) A schematic of the model with matching variables.*

3.2 Forces in STM manipulation

Journal Pre-proof

Scanning probe forces are typically modelled as either purely electrostatic, or electrostatic in combination with short range van der Waals interactions [7]. If purely electrostatic forces from the STM tip were stretching the graphene there would be no displacement at the minimum voltage difference, since $F_{elec.}$ is proportional to the square of the applied voltage difference between the tip and sample [28]. However we are still able to deflect few layer (n=6) graphene more than 70 nm with just ±0.01 V applied to the tip. We cannot measure the tunneling current at V=0 to confirm graphene extension, but we can stop the tip movement in region C of Fig. 1c while the graphene is deflected up towards the tip. If the tip bias is set to zero for several seconds in this region, while the tip is stationary, re-application of the tip bias confirms via the tunneling current magnitude that the same number of graphene layers remained attached to the probe even at V=0. Since extension does not go to zero as V→0, we confirm the presence of short-range van der Waals interactions. The contact potential difference would shift this voltage minimum, discussed later, but we find no point of the response where the displacement goes to zero.

We thus construct a force-balance model which assumes the tip exerts both attractive van der Waals forces F_{vdW} and electrostatic forces $F_{Elec.}$. Bias voltage V is applied to a conducting tip with radius of curvature a. The bias voltage drops across the tunneling gap with resistance R_T and the graphene with resistance R_G, connected in series, to generate tunneling current between the tip and graphene. The presence of attractive forces deflects a stretched graphene membrane of stiffness k out of plane towards the tip, producing a restoring elastic force $F_{Elastic}$ acting on the graphene towards the substrate, as shown in the schematic in Fig. 1d. More information is available in the Supplementary Data File (see Appendix A).

A typical example of the model response is shown in Fig. 2 with the graphene displacement d_1 against the tip-graphene distance at rest, $d=d_0+d_1$, or the tip height. The strongly non-linear dependence of the tunnel current on distance, together with the nonlinearity of van der Waals and elastic forces and linear elastic feedback, produces typical curves on the (d,$d1$) plane that are hysteretic. On approach with d decreasing from infinity the tip follows the lowest stable solution on the blue section marked A. At point B the solution branch terminates, and the graphene discontinuously hops to the yellow diagonal, where $d_1=d$. This is the situation in which the graphene is deflected all the way up to the STM tip, and it is possible to move up and down the diagonal in the model with the graphene attached to the tip. The blue dashed line corresponds to an unstable solution of the model. Retraction follows the diagonal along C before at point D the dashed unstable solution intersects the yellow diagonal. In retraction, crossing this unstable solution causes another discontinuous hop back to the blue line of the stable solution, before moving into region E. We are thus able to use the model to evaluate the width of the hysteretic response Δd which corresponds to the stretch of the graphene before the restoring elastic forces detach it from the tip.

Journal Pre-proof

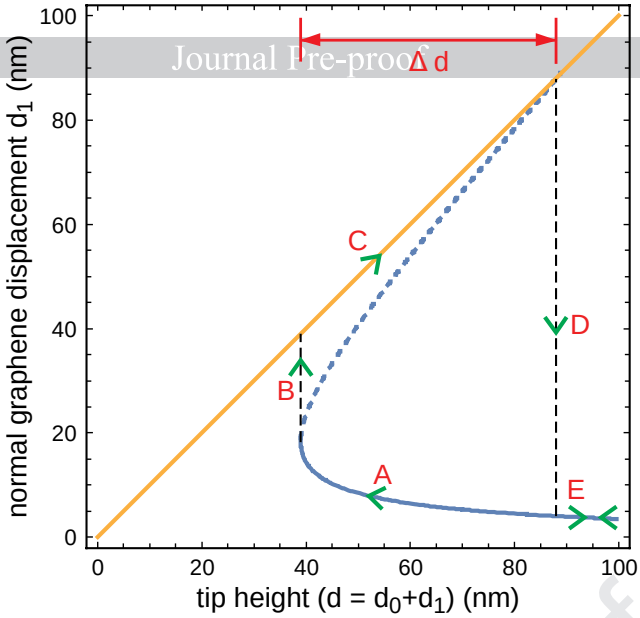

Fig. 2. *Example of a hysteretic response from the force-balance model showing the normal displacement of the graphene d_1 against the tip-graphene distance at rest, d. Labels match the experimental data in Fig. 1.*

3.3 Voltage-dependent manipulation

To understand the mechanical response of the graphene to the STM tip, we examine how this maximum displacement *Δd* depends on tip voltages from −2 to +2 V at room temperature. Repeated approach-retraction measurements are taken at the same position over the void at each voltage and on a portion of the same flake supported by the substrate. The same method is then also applied to a thicker multi-layer (n~8) graphene sample. Combining over one hundred approach-retraction measurements per sample location, Fig. 3 shows the voltage dependence of the maximum graphene displacement against voltage. We note no significant variability in these measurements over time at the same voltage, explored in more detail in the Supplementary Data File, Appendix A.

Within the range (−2, 2) V we observe experimentally three principal forms of graphene stretch against voltage: concave in Fig. 3a, convex in Fig. 3d and a mixture of the two in Fig. 3b and c. In three of the samples the data show that the minimum stretch is not when V→0, and in Fig. 3d increasing the voltage reduces how far the graphene can be stretched up to the measured voltage range. All experimental mean stretches are reasonably symmetric along V=0, discussed later. While the suspended multi-layer (n~8) graphene can be stretched by around 80 nm (Fig. 3d), the portion of the same flake supported on the SiO_2 substrate cannot be stretched beyond 20 nm (Fig. 3c).

Journal Pre-proof

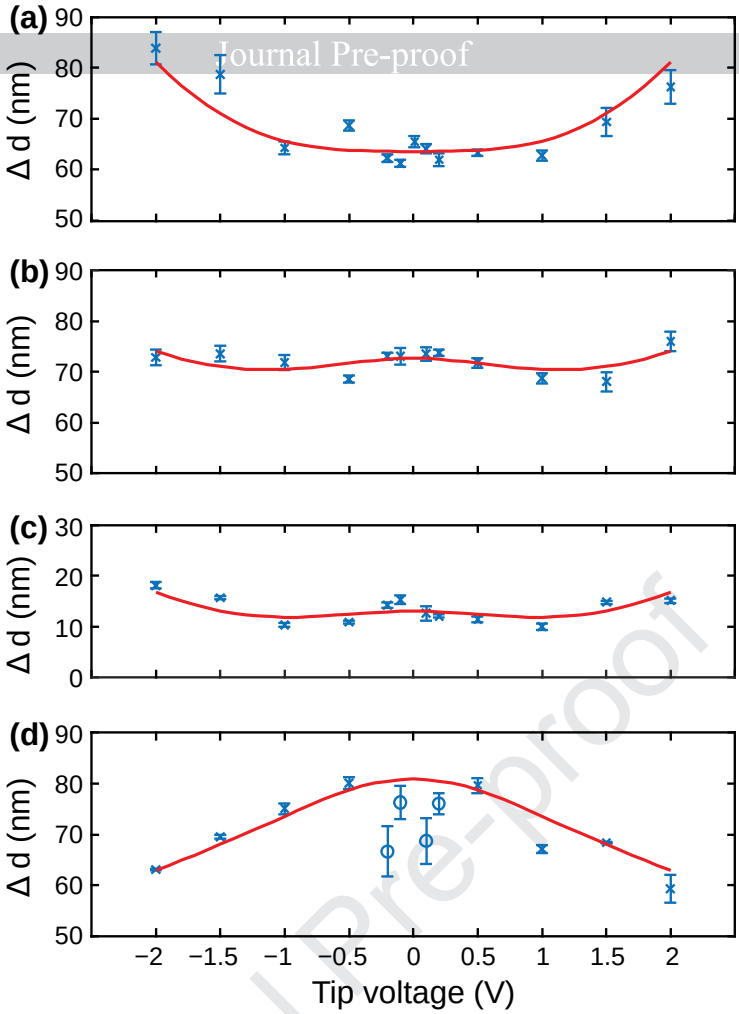

Fig. 3. *Mean graphene displacement from the initial upward deflection to the point at which the graphene fully detaches from the probe (Δd) with standard error: (a) few-layer (n=6) supported (b) few-layer suspended (c) multi-layer (n~8) supported and (d) multi-layer suspended. An example modelled response is overlaid for each dataset as solid lines.*

Journal Pre-proof

To explore the forces involved we overlay example fits to the data in Fig. 3 as solid lines. To produce these the Hamaker constant is taken to be 17×10^{-20} J and fixed.[29] For fixed Hamaker constant, at $V = 0$ an explicit relation exists for d_{vdW} and the ratio a/k when fitted to the measured Δd for $V \to 0$, with the range of determined k discussed later. We use $d_{\mathrm{Elect.}} = d_{\mathrm{vdW}}$ (see Supplementary Data File, Appendix A) and then the only remaining parameters are the ratio of the graphene resistance to tunneling resistance R_G/R_T and the characteristic tunneling distance d_0. The data for each sample are fitted simultaneously to the model using a least squares method in Matlab, with constraint bounds for R_G/R_T and d_0 of (0.001, 10000) and (0, 2 nm) respectively. We find from the model that all of the fitted forms shown in Fig. 3 are mixed concave-convex, with concave behavior at lower voltage, becoming convex at higher voltage. If the fit to Fig. 3d is increased beyond ±2 V it too takes a convex form at higher voltage.

We can include the contact potential difference (V_{cpd}) between the tip and sample in the model by substituting V in the electrostatic force for $V - V_{cpd}$. This shifts the displacement-voltage curves shown,

along the voltage axis. However, the experimental data all appear to be vertically symmetric along V=0, with no horizontal offset. Since the work function for bulk tungsten is ~4.5 eV, and Kelvin probe methods identify a work function for graphene of ~4.6 eV,[30] we assume that the contact potential between the tungsten tip and graphene sample is too small to be evident with this method, and take $V_{cpd} = 0$ in the model.

To explore the origin of these forms we model in Fig. 4 the two attractive tip forces for the suspended few-layer case. The forces change as a function of the tip height *d*, and thus the magnitude of the exerted forces change throughout the hysteresis curve. We examine first in Fig. 4a the point on the hysteresis curve just before the graphene discontinuously deflects up to meet the approaching probe at point B. Forces are normalized to the maximum force to remove the scaling effect of the tip radius, giving the relative contribution, and are shown as a function of tip voltage.

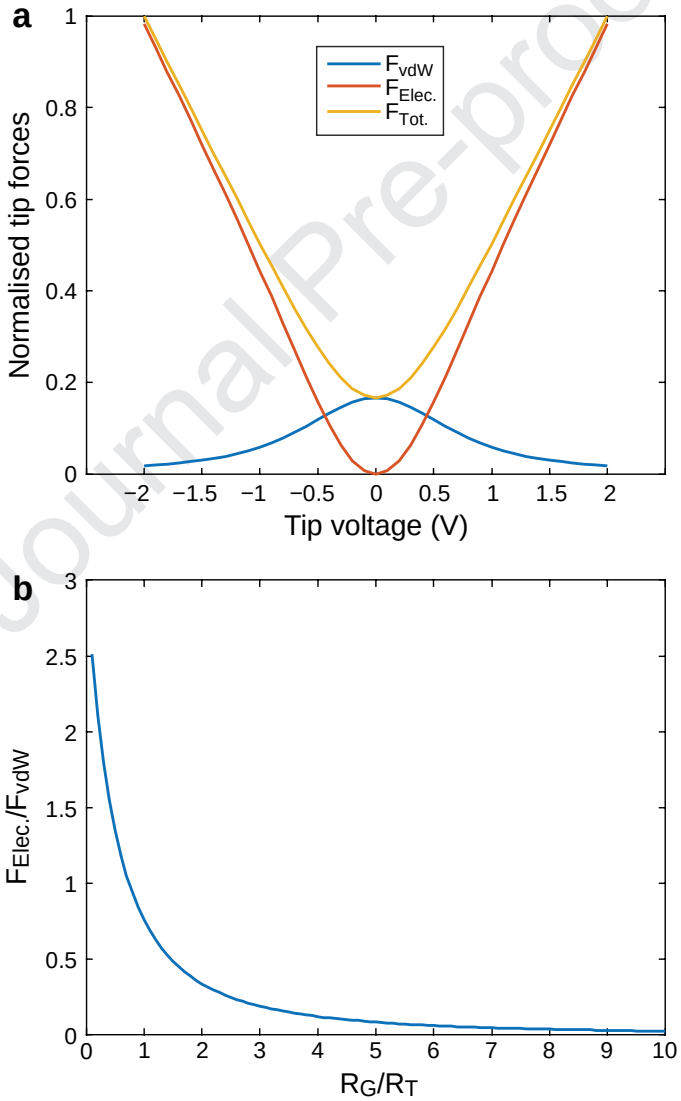

Fig. 4. *Calculated van der Waals and electrostatic forces between the tip and graphene, modelled for the suspended few-layer (n=6) graphene case (a) as a function of voltage just before the graphene discontinuously deflects up to the probe on approach at point B in schematic, and (b) the ratio of the two*

forces once the graphene is 'attached' to the tip (region C in schematic) at bias V = ±2 V as a function of the graphene to tunneling resistance ratio.

Journal Pre-proof

The van der Waals force itself is not voltage dependent, however the interplay of the two distance-dependent forces alters how close the tip must get to the graphene before it discontinuously deflects up to meet the tip. With purely short range van der Waals forces the tip must get closer to induce the upward deflection. As electrostatic forces are added in at higher voltage, these longer-range forces can manipulate the graphene to snap upwards from further away, where the van der Waals force is now lower. This gives rise to a voltage dependence of the initial graphene deflection. However at this point (B) the forces are only weakly dependent on R_G/R_T, and within physically realistic limits practically independent, discussed in the Supplementary Data File (see Appendix A).

Once the graphene has snapped up to the tip, along diagonal C we find a different force relationship during retraction. With the tip-graphene distance fixed there is no longer any voltage or resistance dependence for F_{vdW}. However, the electrostatic force is dependent on both the voltage and the resistance ratio R_G/R_T. In Fig. 4b the ratio of the two forces at fixed bias $V = \pm 2\ V$ is plotted as a function of this resistance ratio. In determining how far the graphene can be stretched, when $R_G/R_T \sim > 1$ the van der Waals force dominates and for $R_G/R_T \sim < 1$ the electrostatic force is higher. For $R_G/R_T < 1$ the same convex form evident at higher voltage is observed down to $V=0$; electrostatic forces dominate. For $R_G/R_T \sim 1$ a concave parabolic response becomes evident at low voltage as seen in Fig. 3a and b where both forces are of similar magnitude. For $R_G/R_T > 1$ the low voltage concave response remains prominent at higher voltages; the van der Waals force dominates. This explains the forms observed experimentally in Fig. 3. Physically, R_T would change between experiments if the tip-graphene distance changed, while the most likely cause of R_G changing between samples would be from the graphene inter-layer separation [6].

One exception to this is the low voltage behavior when $|V| < 0.5$ V for multi-layer graphene suspended over a void in Fig. 3d. These outlying points indicated as circles rather than crosses exhibit a different response and are not included in the fit shown. Although we do not model it, this may be an effect of layer separation. If the layers were separated in this multi-layer (n~8) suspended sample, the short range vdW forces which dominate at low voltage may not penetrate through all the layers, resulting in less graphene stretch than the model fit indicates, and explaining the increased variability.

At V=0 the van der Waals deflection of the membrane is governed largely by the stiffness of the graphene k. Our model does not directly include the number of layers of graphene, but could account for this via a change in the stiffness. Our model can only determine the ratio a/k, but since the same tip with the same effective radius of curvature a is used throughout, it is considered constant. Assuming the tip radius of curvature a = 100 nm, and typical values of the other constants, the fits shown in Fig. 3 use values of stiffness k from 0.05 Nm^{-1} to 0.075 Nm^{-1}. These are lower than typically reported values of 1 – 5 Nm^{-1}

using AFM to indent few-layer graphene [31], for which there are several possible reasons. AFM indentation measurements record values of *k* which reduce away from the edge of the void towards a minimum when suspended graphene is furthest from boundary clamping [31]. Our method lifts the graphene away from the surface and if the graphene-substrate forces which create the boundary clamping were reduced, we may measure lower values of *k*. If after deposition there is slack in the graphene layers, this too would reduce the apparent stiffness [8].

Mashoff *et al* used STM to apply AC voltages to graphene to measure deflection in a similar way [7]. From a stable reference position with the tip remaining in contact with the graphene, their measurements of Δz were relative to this reference position with $\Delta z=0$ when the applied voltage was equal to the voltage used to establish the initial contact condition with a maximum deflection measured < 0.1 nm. We are instead establishing a new reference position for each voltage. We are able to determine here the interplay of both the van der Waals and electrostatic forces in determining that starting deflection position, as well as the maximum possible displacement away from it until restoring elastic forces detach the graphene from the probe.

Like all scanning probe measurements the nature of the probe-sample interaction is often understood in combination with simulation [32, 33]. STM has been used to apply stress-strain tests to graphene membranes, with the applied force calculated instead of measured, by assuming only electrostatic forces modified by the tunneling distance [8]. Here we show that such calculations would need to include the van der Waals force as well for low voltage, with typical STM tip-sample distances. Other work assumes that electrostatic and van der Waals interactions are present [34], but here we show that changes in the graphene resistance can alter the relative contribution of these forces.

By applying a back-gated voltage, doubly-clamped graphene beams can be manipulated between two meta-stable hysteretic states in the same way as the local manipulation induced using STM [9]. With cavity spacings on the order of 100 nm, purely long-range electrostatic interactions drive this switch. However, when the deflection of the beam or membrane is close to the size of the cavity, short-range van der Waals forces from the cavity bottom can affect device performance [16]. STM manipulation could be applied to study these effects in graphene suspended over cavities of different depths.

4. Conclusion

Two-probe scanning tunneling microscopy has been used to stretch few- (n=6) and multi-layer (n~8) graphene membranes supported on SiO_2 and suspended over holes, in ultra high vacuum, without lithographically fabricated contacts. Stretching the graphene membranes using the probe follows the reported hysteretic response between the in-contact and maximum extension states, but we find the membrane extension depends on voltage. Using a scripted approach-retraction method hundreds of hysteresis curves are traced repeatedly at constant speed, with the extension extracted as a function of

Journal Pre-proof

voltage. We fit the measured data to a model which balances the attractive electrostatic and van der Waals interactions of the probe against the elastic graphene membrane, replicating the hysteretic behavior of stretched graphene membranes. We find a complex concave-convex response where the influence of the two forces is dependent on the sample and substrate properties.

Journal Pre-proof

This work shows how competing substrate forces with layered graphene can alter the voltage dependence of local probe manipulation, and is applicable in cavity structures such as oscillators where side walls exert both electrostatic and short-range forces on the graphene membranes. Such a method could be used to control the path of electrons through multi-layered 2D structures by locally altering layer spacing, and with the resulting control over capacitance it offers a potential mechanism for voltage switching [35]. These results not only inform scanning probe measurements of graphene, but controlling local perturbations in graphene and other 2D materials is expected to lead to strain engineered materials [1].

Appendix A. Supplementary data

Supplementary data to this article can be found online at …

References

[1] V.M. Pereira, A.H. Castro Neto, Strain Engineering of Graphene's Electronic Structure, Physical Review Letters 103(4) (2009) 046801.
[2] F.R. Eder, J. Kotakoski, K. Holzweber, C. Mangler, V. Skakalova, J.C. Meyer, Probing from Both Sides: Reshaping the Graphene Landscape via Face-to-Face Dual-Probe Microscopy, Nano Letters 13(5) (2013) 1934-1940.
[3] D. Zhai, N. Sandler, Local versus extended deformed graphene geometries for valley filtering, Physical Review B 98(16) (2018) 165437.
[4] A.K. Geim, I.V. Grigorieva, Van der Waals heterostructures, Nature 499 (2013) 419.
[5] M. Neek-Amal, P. Xu, J.K. Schoelz, M.L. Ackerman, S.D. Barber, P.M. Thibado, A. Sadeghi, F.M. Peeters, Thermal mirror buckling in freestanding graphene locally controlled by scanning tunnelling microscopy, Nature Communications 5 (2014) 4962.
[6] M.M.M. Alyobi, C.J. Barnett, P. Rees, R.J. Cobley, Modifying the electrical properties of graphene by reversible point-ripple formation, Carbon 143 (2019) 762-768.
[7] T. Mashoff, M. Pratzer, V. Geringer, T.J. Echtermeyer, M.C. Lemme, M. Liebmann, M. Morgenstern, Bistability and Oscillatory Motion of Natural Nanomembranes Appearing within Monolayer Graphene on Silicon Dioxide, Nano Letters 10(2) (2010) 461-465.
[8] B. Uder, H. Gao, P. Kunnas, N. de Jonge, U. Hartmann, Low-force spectroscopy on graphene membranes by scanning tunneling microscopy, Nanoscale 10(4) (2018) 2148-2153.
[9] N. Lindahl, D. Midtvedt, J. Svensson, O.A. Nerushev, N. Lindvall, A. Isacsson, E.E.B. Campbell, Determination of the Bending Rigidity of Graphene via Electrostatic Actuation of Buckled Membranes, Nano Letters 12(7) (2012) 3526-3531.
[10] N.N. Klimov, S. Jung, S. Zhu, T. Li, C.A. Wright, S.D. Solares, D.B. Newell, N.B. Zhitenev, J.A. Stroscio, Electromechanical Properties of Graphene Drumheads, Science 336(6088) (2012) 1557-1561.

[11] S. Tsoi, P. Dev, A.L. Friedman, R. Stine, J.T. Robinson, T.L. Reinecke, P.E. Sheehan, van der Waals Screening by Single-Layer Graphene and Molybdenum Disulfide, ACS Nano 8(12) (2014) 12410-12417.
[12] F. Guan, X. Du, Random Gauge Field Scattering in Monolayer Graphene, Nano Letters 17(11) (2017) 7009-7014.
[13] G.G. Naumis, S. Barraza-Lopez, M. Oliva-Leyva, H. Terrones, Electronic and optical properties of strained graphene and other strained 2D materials: a review, Reports on Progress in Physics 80(9) (2017) 096501.
[14] H. Rokni, W. Lu, Surface and Thermal Effects on the Pull-In Behavior of Doubly-Clamped Graphene Nanoribbons Under Electrostatic and Casimir Loads, Journal of Applied Mechanics 80(6) (2013) 061014-061014-9.
[15] N. Inui, Casimir effect on graphene resonator, Journal of Applied Physics 119(10) (2016) 104502.
[16] C. Berger, R. Phillips, A. Centeno, A. Zurutuza, A. Vijayaraghavan, Capacitive pressure sensing with suspended graphene–polymer heterostructure membranes, Nanoscale 9(44) (2017) 17439-17449.
[17] Y. Sui, J. Appenzeller, Screening and Interlayer Coupling in Multilayer Graphene Field-Effect Transistors, Nano Letters 9(8) (2009) 2973-2977.
[18] Y. Ni, Y. Chalopin, S. Volz, Significant thickness dependence of the thermal resistance between few-layer graphenes, Applied Physics Letters 103(6) (2013) 061906.
[19] M. Ishigami, J.H. Chen, W.G. Cullen, M.S. Fuhrer, E.D. Williams, Atomic Structure of Graphene on SiO2, Nano Letters 7(6) (2007) 1643-1648.
[20] A. Jacobsen, F.M. Koehler, W.J. Stark, K. Ensslin, Towards electron transport measurements in chemically modified graphene: effect of a solvent, New Journal of Physics 12(12) (2010) 125007.
[21] M. Morgenstern, N. Freitag, A. Nent, P. Nemes-Incze, M. Liebmann, Graphene Quantum Dots Probed by Scanning Tunneling Microscopy, Annalen der Physik 529(11) (2017) 1700018.
[22] M.B. Klarskov, H.F. Dam, D.H. Petersen, T.M. Hansen, A. Löwenborg, T.J. Booth, M.S. Schmidt, R. Lin, P.F. Nielsen, P. Bøggild, Fast and direct measurements of the electrical properties of graphene using micro four-point probes, Nanotechnology 22(44) (2011) 445702.
[23] C.J. Barnett, G. Jackson, D.R. Jones, A.R. Lewis, K. Welsby, J.E. Evans, J.D. McGettrick, T. Watson, T.G.G. Maffeis, P.R. Dunstan, A.R. Barron, R.J. Cobley, Investigation into the effects of surface stripping ZnO nanosheets, Nanotechnology 29(16) (2018) 165701.
[24] A.M. Lord, T.G. Maffeis, O. Kryvchenkova, R.J. Cobley, K. Kalna, D.M. Kepaptsoglou, Q.M. Ramasse, A.S. Walton, M.B. Ward, J. Köble, S.P. Wilks, Controlling the Electrical Transport Properties of Nanocontacts to Nanowires, Nano Letters 15(7) (2015) 4248-4254.
[25] M.M.M. Alyobi, C.J. Barnett, R.J. Cobley, Effects of Thermal Annealing on the Properties of Mechanically Exfoliated Suspended and On-Substrate Few-Layer Graphene, Crystals 7(11) (2017) 349.
[26] R.J. Cobley, R.A. Brown, C.J. Barnett, T.G.G. Maffeis, M.W. Penny, Quantitative analysis of annealed scanning probe tips using energy dispersive x-ray spectroscopy, Applied Physics Letters 102(2) (2013) 023111.
[27] N.A. Smith, A.M. Lord, J.E. Evans, C.J. Barnett, R.J. Cobley, S.P. Wilks, Forming reproducible non-lithographic nanocontacts to assess the effect of contact compressive strain in nanomaterials, Semiconductor Science and Technology 30(6) (2015) 065011.
[28] K. Wang, J. Cheng, S. Yao, Y. Lu, L. Ji, D. Xu, Determination of electrostatic force and its characteristics based on phase difference by amplitude modulation atomic force microscopy, Nanoscale Res Lett 11(1) (2016) 548-548.
[29] Y.-C. Chiou, T.A. Olukan, M.A. Almahri, H. Apostoleris, C.H. Chiu, C.-Y. Lai, J.-Y. Lu, S. Santos, I. Almansouri, M. Chiesa, Direct Measurement of the Magnitude of the van der Waals Interaction of Single and Multilayer Graphene, Langmuir 34(41) (2018) 12335-12343.
[30] Y.-J. Yu, Y. Zhao, S. Ryu, L.E. Brus, K.S. Kim, P. Kim, Tuning the Graphene Work Function by Electric Field Effect, Nano Letters 9(10) (2009) 3430-3434.
[31] I.W. Frank, D.M. Tanenbaum, A.M. Van der Zande, P.L. McEuen, Mechanical properties of suspended graphene sheets, Journal of Vacuum Science & Technology B 25(6) (2007) 2558-2561.
[32] O. Kryvchenkova, R.J. Cobley, K. Kalna, Self-consistent modelling of tunnelling spectroscopy on III–V semiconductors, Applied Surface Science 295 (2014) 173-179.
[33] O. Kryvchenkova, I. Abdullah, J.E. Macdonald, M. Elliott, T.D. Anthopoulos, Y.-H. Lin, P. Igić, K. Kalna, R.J. Cobley, Nondestructive Method for Mapping Metal Contact Diffusion in In2O3 Thin-Film Transistors, ACS Applied Materials & Interfaces 8(38) (2016) 25631-25636.
[34] R. Breitwieser, Y.-C. Hu, Y.C. Chao, Y.R. Tzeng, S.-C. Liou, K.C. Lin, C.W. Chen, W.W. Pai, Investigating ultraflexible freestanding graphene by scanning tunneling microscopy and spectroscopy, Physical Review B 96(8) (2017) 085433.
[35] R.D. Yamaletdinov, O.V. Ivakhnenko, O.V. Sedelnikova, S.N. Shevchenko, Y.V. Pershin, Snap-through transition of buckled graphene membranes for memcapacitor applications, Scientific Reports 8(1) (2018) 3566.

Journal Pre-proof

Mona Alyobi: Experimentation, Writing. Chris Barnett: Experimentation. Cyrill Muratov: Modeling, Writing. Vitaly Moroz: Modeling, Writing. Richard Cobley: Experimentation, Modeling, Writing, Supervision.

Journal Pre-proof

Journal Pre-proof

Declaration of interests

☒ The authors declare that they have no known competing financial interests or personal relationships that could have appeared to influence the work reported in this paper.

☐The authors declare the following financial interests/personal relationships which may be considered as potential competing interests:

Journal Pre-p